AD-A098 719 FLORIDA STATE UNIV TALLAHASSEE F/G 20/4
NUMERICAL COMPUTATION OF LARGE AMPLITUDE INTERNAL SOLITARY WAVE--ETC(U)
MAR 81 T F CHAN N00014-80-C-0076
UNCLASSIFIED 198 NL

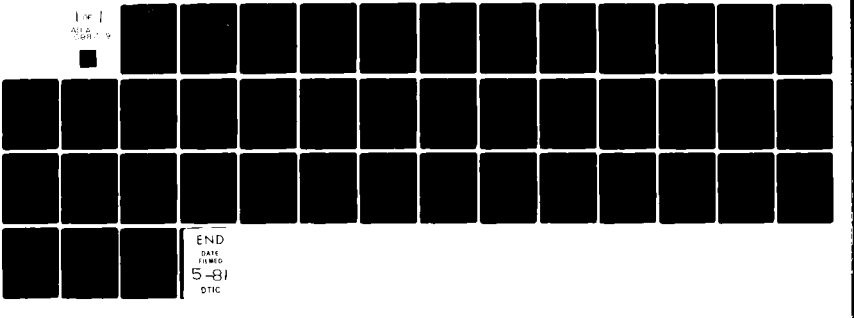

END
DATE FILMED
5-81
DTIC

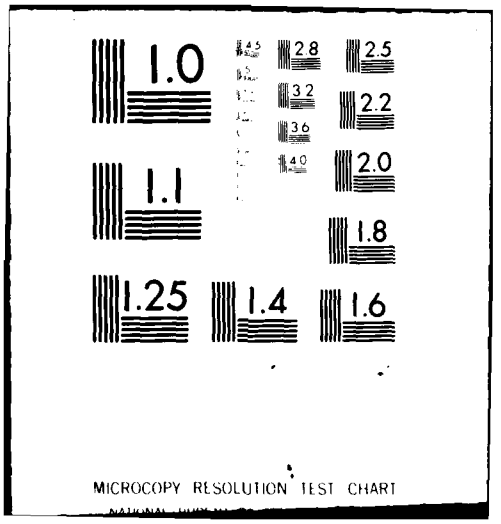
1.0
1.1
1.25
1.4
1.6
1.8
2.0
2.2
2.5
2.8
3.2
3.6
4.0
MICROCOPY RESOLUTION TEST CHART

LEVEL II

12

Contract N00014-80-C-0076

YALE UNIVERSITY
DEPARTMENT OF COMPUTER SCIENCE

(12)

(14) 198

(12) 43

(15) N00014-80-C-0076

(6) NUMERICAL COMPUTATION OF LARGE AMPLITUDE INTERNAL SOLITARY WAVES,

(10) Tony F.C. Chan #198

Computer Science Department

Yale University

(11) 20 Mar 81

139850

ABSTRACT

Finite amplitude internal solitary waves in a stratified fluid are computed numerically as solutions to a version of Long's equation [16]. Newton's method is used to linearize the two dimensional nonlinear elliptic equation and numerical continuation techniques, both using the wave speed and a pseudo-arclength parameter, are used to trace out solution branches efficiently. Numerical results for the 'tanh' density profile are presented here for various depths of the fluid. For shallow depths, solutions for a fixed wave speed are not unique and bore-like solutions with large amplitude have been found. In the deep water case, excellent agreement is obtained with the experimental data of Davis and Acrivos [9] whereas traditional weakly nonlinear analysis fails to produce agreement in the large amplitude regime.

[1]This work was supported by Dynamics Technology Inc., Torrance, California and by ONR Grant N00014-80-0076 under subcontract from Florida State University.

Table of Contents

1. Introduction

Large amplitude internal waves which maintain their shape over long distance of propagation (hence the name 'solitary') are often observed in nature and have recently been suggested to occur in the Jovian atmosphere in the form of the Great Red Spots [18]. These waves can also be generated in the laboratory rather easily [17], which suggests that they can be excited under many circumstances in natural systems. Most of the existing theories ([5], [6], [14], [20]), with a few exceptions([2]), are limited to the case of small amplitude and long wavelengths, due to analytical difficulties. The small amplitude assumption allows the solution to be expressed in an asymptotic expansion in terms of the amplitude and the nonlinear governing equations to be solved by perturbation techniques. The long wavelength assumption reduces the governing two dimensional partial differential equation into ordinary differential equations. In applications, results from these weakly nonlinear theories are often extrapolated into the large amplitude and short wavelength domains. While it is remarkable that such extrapolations agree quite favorably with experimental data even for moderately large wave amplitudes and short wavelengths, notable discrepancies exist both quantitatively and qualitatively in many situations.

In this paper, we tackle numerically the original nonlinear partial differential equation directly without making either the small amplitude

assumption or the long wavelength assumption. Large amplitude waves with short wavelengths have been computed together with the small amplitude and long wavelength ones. The nonlinear equation is linearized by Newton's method and the resulting linear equations are discretized by standard finite difference methods. In the deep fluid cases, the waves only occupy a small portion of the computational domain, and use of uniform mesh spacing would be wasteful. Our solution is to use an analytical transformation of the domain so that a uniform mesh in the transformed domain gives adequate resolution without too much waste. The governing equation contains a physical parameter : the wave speed, and we are interested in computing many different waves corresponding to different wave speeds. To make the computational process more efficient, we employ continuation techniques (with respect to the wave speed) whereby known solution at a given wave speed can provide extremely good initial guess for Newton's method at a nearby wave speed. Moreover, in a shallow fluid case we found nonunique solutions for a given wave speed. In order to provide a systematic way to trace some of these nonunique solutions, an arclength continuation technique [12] is employed.

In Section 2, the governing partial differential equations are discussed, and in Section 3 , a description of Newton's method and the continuation techniques is given. Details of numerical implementation are described briefly in Section 4, and numerical results and comparison with experimental data are

presented in Section 5. The conclusion is in Section 6.

This paper is a companion to the paper by Tung, Chan and Kubota [24]. There we focus on more mathematical issues such as proving existence of large amplitude solutions and relating the dependence of wave amplitude on wave speed to the density profile of the fluid medium. For a more thorough discussion of the fluid dynamical aspects of the waves computed in the current paper and other background information, the reader is referred to the companion paper. The present paper focuses on the numerical techniques used to computed the large amplitude waves. It is hoped that the numerical techniques are of more general interest and can find applications in other areas.

2. Governing Equations

Consider a stably stratified fluid, the ocean for example, which is perturbed and set into motion (Figure 2-1). The interaction of the density variations and the force of gravity can give rise to many interesting wave phenomena. Internal solitary waves are a well-known example [9, 10]. These are waves that propagate inside the fluid, rather than on the surface, and can travel long distances without changing their shape or losing their energy.

The equation that governs the steady state propagation and shape of these internal waves can be derived from the equations of motion of an incompressible, inviscid, and non-diffusive fluid of variable density [16, 24], which, in terms of dimensionless variables for the case of uniform mean flow, is:

$$\Delta u + \lambda u F'(y+u)/(1-\sigma F(y+u)) = \sigma F'(y+u)(u_x^2 + u_y^2 + 2\, u_y)/(1-\sigma F(y+u))/2, \qquad (2.1)$$

with boundary conditions:

$u = 0$ on the surface and bottom of fluid,

$u \to 0$ as $|x| \to \infty$,

where

Figure 2-1: Internal Solitary Wave Environment

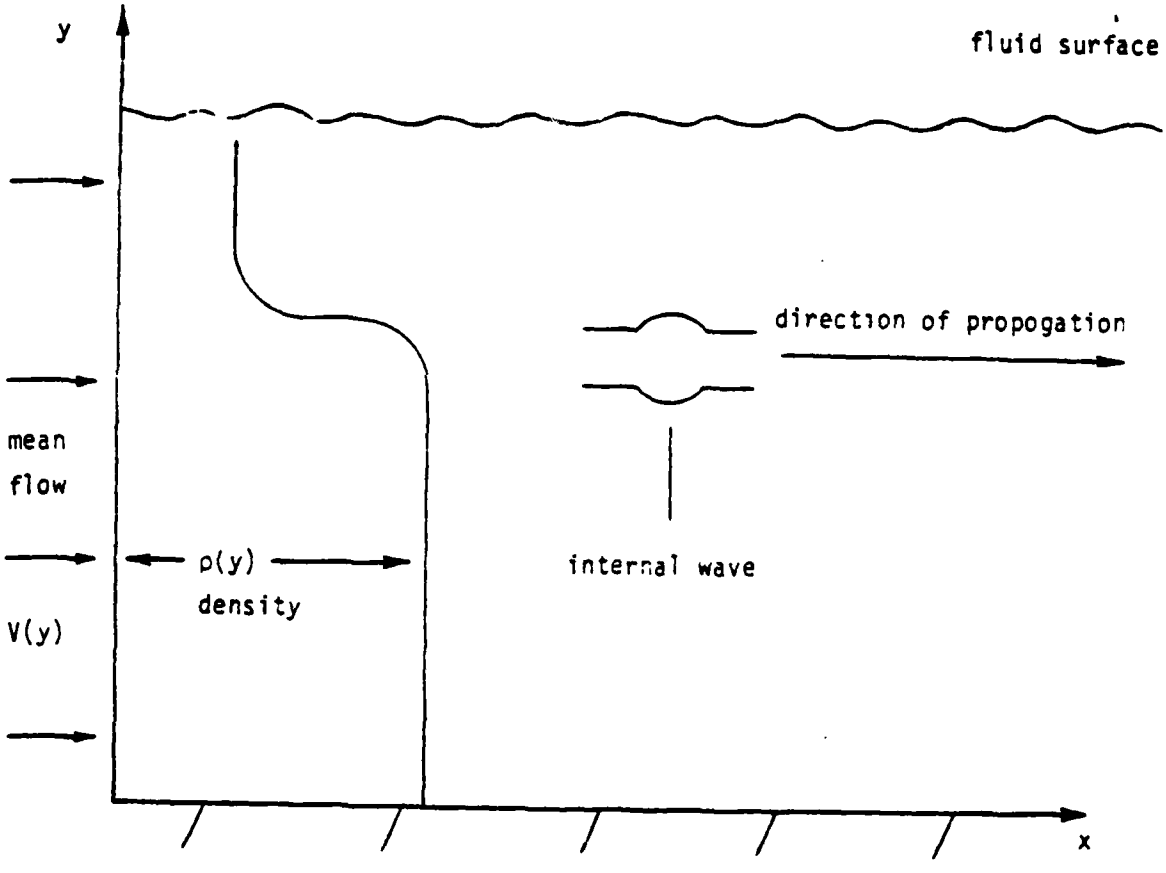

- u is the perturbation stream function,

- λ is a nondimensional quantity inversely proportional to the square of the wave speed,

- ρ the density is given by:

$$\rho = \rho_0(1 - \sigma F(y+u)), \tag{2.2}$$

where F is a given nonlinear function that specifies the density stratification profile; an often used profile is the 'tanh'-profile: $F(y) = \tanh(y)$,

- σ can be interpreted as the relative density change across the entire stratified layer.

Equation (2.1) is seldom solved in this complicated and fully nonlinear form. Often the relative density stratification is very small (e.g. in the ocean), so that $\sigma << 1$ and the so-called Boussinesq approximation is made. Equation (2.1) is then reduced to the simpler form, to which we shall refer to as Long's Equation [16]:

$$\Delta u + \lambda F'(y+u)\, u = 0. \tag{2.3}$$

Equation (2.3) is the equation we will be dealing with in this paper. For the purpose of describing the numerical methods in the next section, it is

convenient to write Equation (2.3) formally as

$$G(u , \lambda) = 0 \qquad (2.4)$$

to show the dependence of the perturbation stream function u on the parameter λ. Equation (2.4) is in the form of a nonlinear elliptic eigenvalue problem [4, 12].

3. Newton's Method and Continuation Techniques

3.1 Newton's Method

Solving a nonlinear eigenvalue problem $G(u,\lambda) = 0$ can take on at least two different meanings:

1. Solve for $u(\lambda)$ given a specific value for λ.
2. Determine the dependence of u on λ.

In this paper, we adopt the second meaning. Clearly, if we have a good procedure for solving Problem (2), we can also use it to solve Problem (1) effectively.

The usual solution procedure for nonlinear problems involves linearization and application of some version of Newton's method.

Newton's Method :

Given a value of λ and an initial guess u^0 for the solution $u(\lambda)$, we perform the following steps repeatedly until satisfied :

$$G_u^i \, \delta u^i = - G(u^i,\lambda) \tag{3.1}$$

$$u^{i+1} = u^i + \delta u^i. \tag{3.2}$$

In the above, subscripts denote partial derivatives and so G_u denotes the Jacobian of the operator G (with respect to u). This procedure will generally

converge quadratically when it does converge. However, as is well known, in many instances it will fail to converge when the initial guess is not 'close' to the true solution.

3.2 Natural Continuation

A plausible procedure for overcoming this convergence difficulty and also for determining the dependence of u on λ is to start at a known solution (u_0,λ_0) on the solution curve and use it as initial guess for a Newton-type iteration to find the solution for a neighboring point on the solution curve with λ close to λ_0 and repeating the procedure. We can improve on this further by computing the 'slope' u_λ at a known solution and use it to get a better initial guess for the next value of λ in a predictor-corrector fashion. We shall call this the Natural Continuation Procedure because it corresponds to parametrizing the solution curve by λ, the naturally occurring parameter.

Natural Continuation Procedure:

Given a known solution (u_0,λ_0), we want to compute the solution at a nearby value of λ.

1. First compute the 'slope' u_λ at (u_0,λ_0) from

$$G_u\, u_\lambda = -\, G_\lambda. \tag{3.3}$$

2. Perform an Euler predictor step:

$$u^0 = u_0 + u_\lambda (\lambda - \lambda_0). \tag{3.4}$$

3. Use u^0 as initial guess in Newton's method for $G(u,\lambda)=0$:

$$G_u^i (u^{i+1} - u^i) = - G(u^i,\lambda) \tag{3.5}$$

until convergence.

4. Use $(u(\lambda),\lambda)$ as the new (u_0,λ_0) and go back to Step 1.

Note that very often the computation of the slope u_λ does not cause much computational overhead because we usually have the factorization of the Jacobian G_u computed already in the Newton step. Using the slope in a predictor-corrector fashion will often allow us to take a much bigger step in λ and thus reduce the overall cost of determining the dependence of u on λ.

Unfortunately, this procedure needs some modification in order to handle general nonlinear systems because of the possibility of existence of nonunique solutions. The nonuniqueness usually manifests itself in the form of existence of 'singular' points where the Jacobian G_u is singular (see Figure 3-1). Points such as point A in Figure 3-1 are called limit points (or turning points) and points such as point B are called bifurcation points. These singular points are further characterized by the conditions that $G_\lambda \notin \text{Range}(G_u)$ at a limit point and that $G_\lambda \in \text{Range}(G_u)$ at a bifurcation point [12].

Figure 3-1: A Typical Bifurcation Diagram

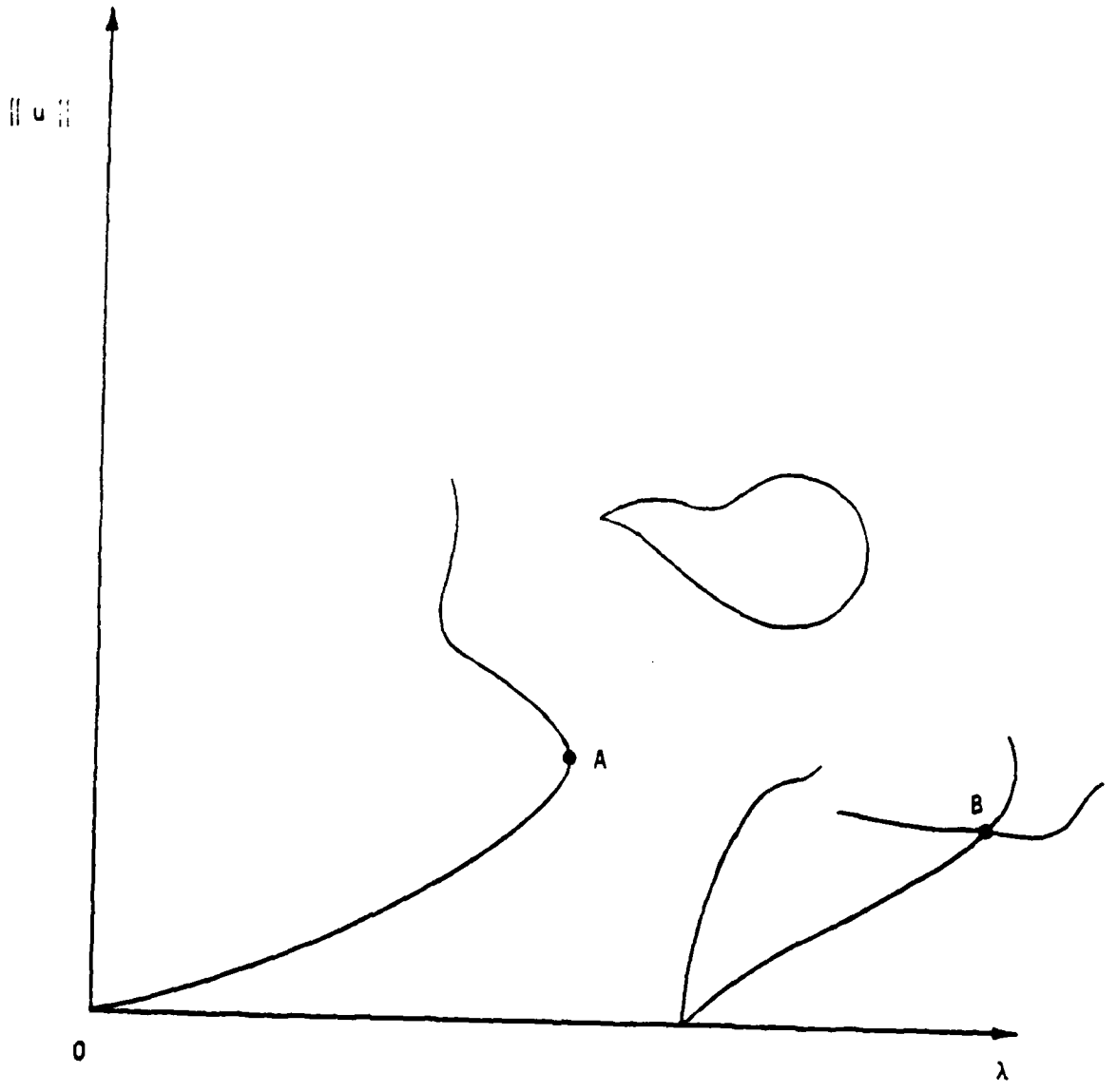

The difficulties that the Natural Continuation Procedure will encounter are three-fold. First of all, since G_u is singular at these points, Newton's method will in general be only linearly convergent, making it much more costly to compute the solution. Moreover, when tracing a solution branch near a limit point, there may not exist a solution for a given value of λ (see Figure 3-2) and hence Equation (3.5) will fail. Lastly, we need some mechanism for switching branches at a bifurcation point.

3.3 Arclength Continuation

In the pseudo-arclength continuation approach [3, 12], this difficulty is overcome by not imposing a value for λ at which the solution $u(\lambda)$ is sought. Instead, we parametrize the solution branches using an arclength parameter s, *and specify* how far along the current solution branch we want to march.

To be more specific, we let s be the arclength parameter, and treat u(s) and $\lambda(s)$ as functions of s. We can compute the 'slopes' $\dot{u}(s_0)$, $\dot{\lambda}(s_0)$ (where the dots denote differentiation with respect to s) of a known solution at $s=s_0$ from the following two equations:

$$G_u \dot{u}_0 + \dot{\lambda}_0 G_\lambda = 0, \tag{3.6}$$

$$||\dot{u}_0||^2 + |\dot{\lambda}_0|^2 - 1 = 0. \tag{3.7}$$

Equation (3.6) is obtained from differentiating $G(u,\lambda) = 0$ with respect to s

Figure 3-2: Failure of Natural Continuation Near Limit Points

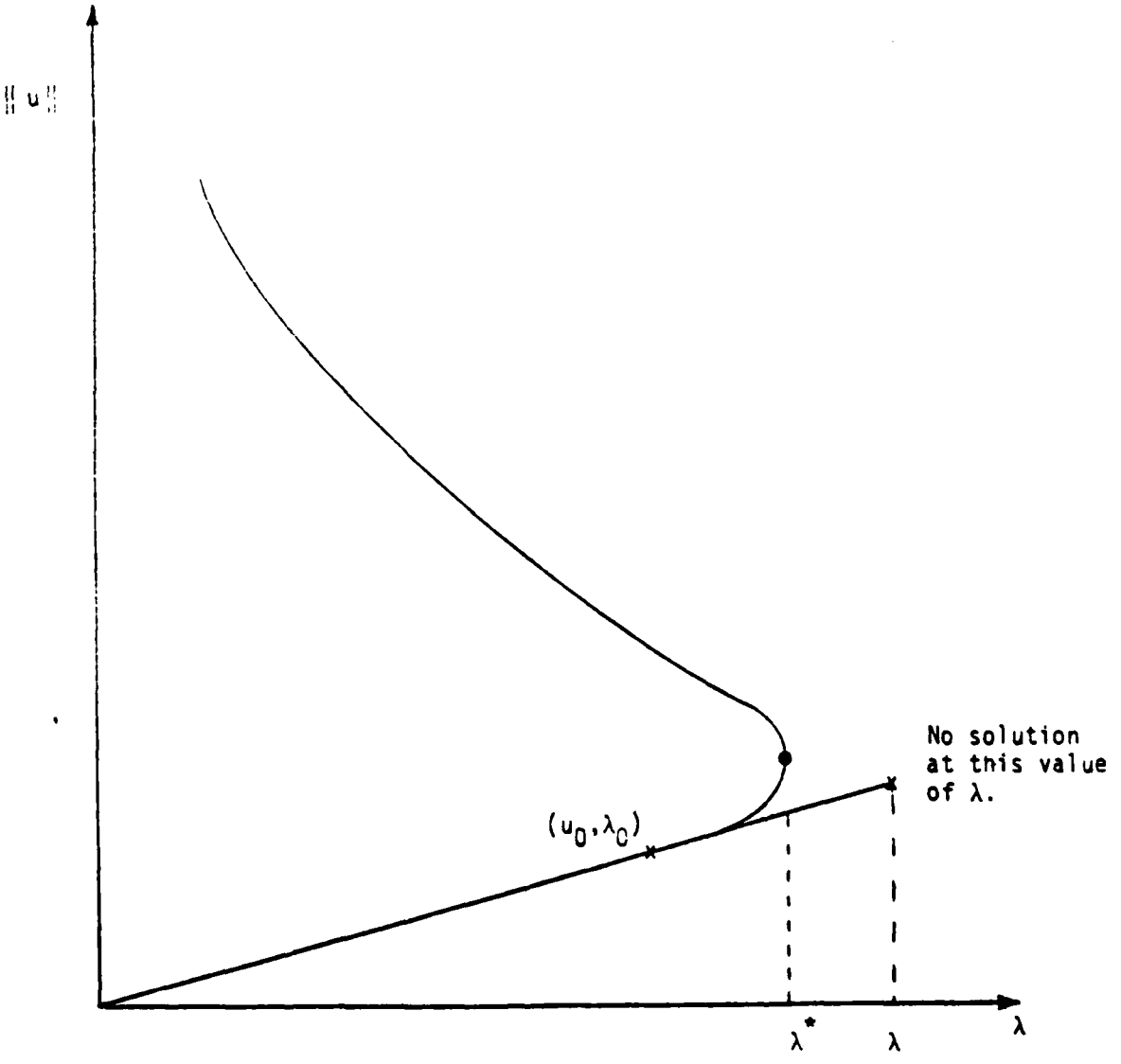

and Equation (3.7) imposes the arclength condition. We can theoretically 'follow' the solution curve by integrating the initial value problem defined by $\dot{u}(s)$ and $\dot{\lambda}(s)$. However, this process may become unstable —— the approximate solution to the initial value problem may deviate more and more from the true solution curve. One way to stabilize this procedure is to use $\dot{u}(s)$ and $\dot{\lambda}(s)$ in a predictor step to provide an initial guess for a Newton-type method to bring it back onto the true solution curve (Figure 3-3).

In the pseudo-arclength continuation procedure, we advance from s_0 to s along the solution branch by requiring the new solution $u(s)$ and $\lambda(s)$ to satisfy the following equations:

$$N(u(s),\lambda(s)) \equiv \dot{u}_0^T(u(s) - u(s_0)) + \dot{\lambda}_0(\lambda(s) - \lambda(s_0)) - (s - s_0) = 0 \quad (3.8)$$

and

$$G(u(s),\lambda(s)) = 0. \quad (3.9)$$

Equation (3.8) is the linearization of Equation (3.7) and essentially forces the new solution to lie on a hyperplane perpendicular to the tangent vector of the solution curve at s_0 and at a distance $(s-s_0)$ from it. Equation (3.9) requires $u(s)$ and $\lambda(s)$ to lie on the true solution curve (Figure 3-3). We now solve the coupled system (3.8) and (3.9) for $u(s)$ and $\lambda(s)$, given the step size $(s-s_0)$ (efficient strategies for choosing the step size are discussed in [21]). We can use Newton's method, in which case we have to solve the

Figure 3-3: Pseudo-Arclength Continuation

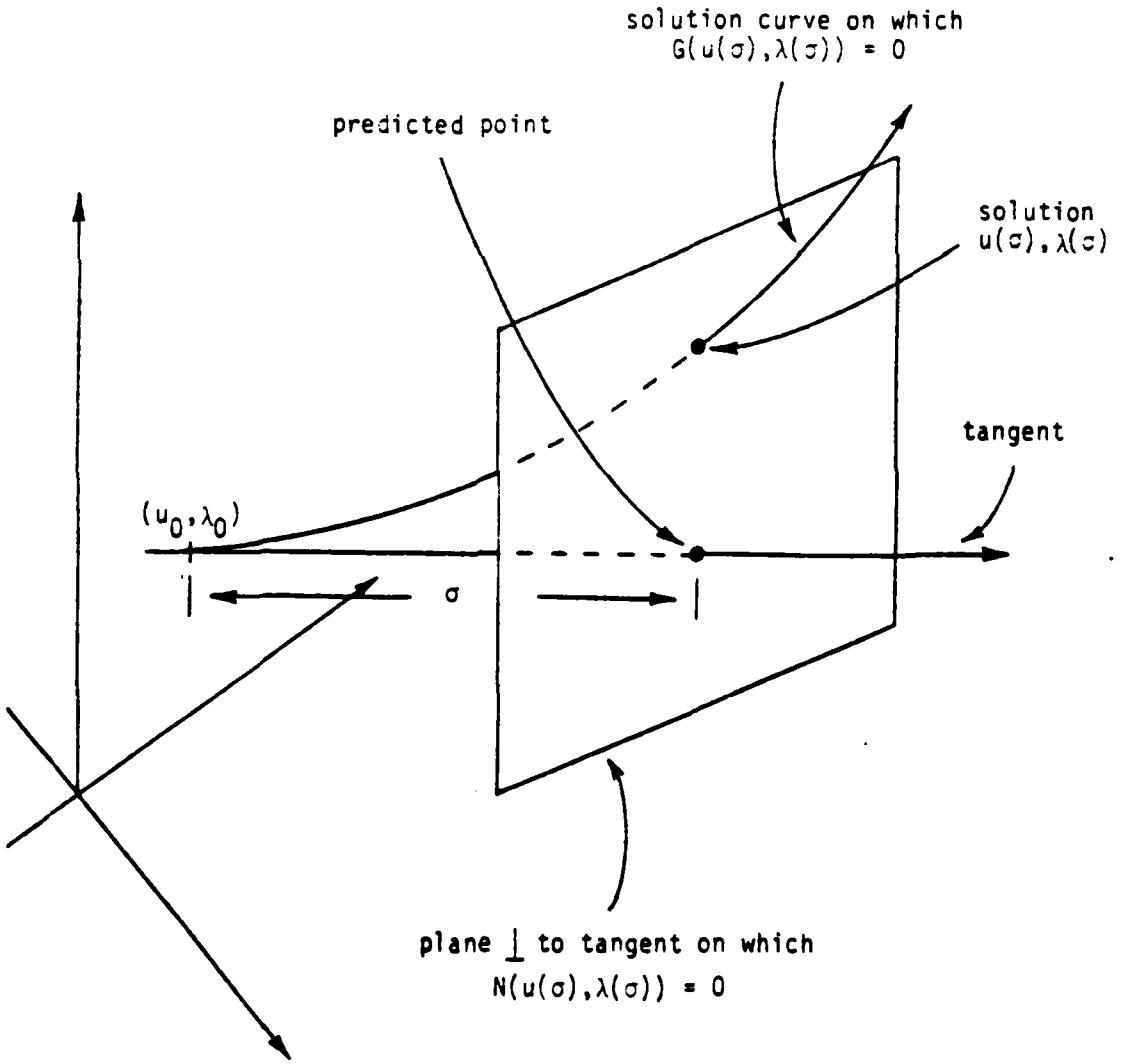

following linear system at each iteration:

$$A \begin{bmatrix} \delta u \\ \delta \lambda \end{bmatrix} = \begin{bmatrix} G_u & G_\lambda \\ N_u^T & N_\lambda \end{bmatrix} \begin{bmatrix} \delta u \\ \delta \lambda \end{bmatrix} = - \begin{bmatrix} G \\ N \end{bmatrix} \tag{3.10}$$

It can be shown that at limit points, where G_u is singular and $G_\lambda \notin \text{Range}(G_u)$, the linear system in Equation (3.10) is nonsingular (see [12]) and therefore Newton's method for the coupled system (3.8) and (3.9) is well-defined. Hence limit points present no problem and even quadratic convergence is achievable.

At bifurcation points, where G_u is singular and $G_\lambda \in \text{Range}(G_u)$, things are more complicated. In the simplest case of only one branch bifurcating from the main branch (simple bifurcation), an additional higher order condition (see for example Crandall and Rabinowitz [8]) involving G_{uu}, $G_{u\lambda}$ and $G_{\lambda\lambda}$ has to be satisfied. It can be shown [12] that this condition, together with Equations (3.6) and (3.7) and the left and right null vectors of G_u, enable two solutions for $(\dot{u}_0, \dot{\lambda}_0)$ to be computed at a simple bifurcation point, with one solution corresponding to each branch. Using the appropriate pair of $(\dot{u}_0, \dot{\lambda}_0)$ in Equation (3.8) allows branch switching.

In order to solve the linear system in Equation (3.10) by direct methods,

several approaches are possible. One way is to perform Gaussian elimination on the inflated matrix A, with some form of pivoting to insure stability. But this approach completely ignores the sparse structure which is usually found in G_u's arising from nonlinear elliptic eigenvalue problems. In order to take advantage of the structure in G_u, Keller [12] suggested the following block-elimination procedure:

Algorithm BE: (block-elimination)

Solve $$G_u\, y = G_\lambda \tag{3.11}$$

and $$G_u\, z = -\, G. \tag{3.12}$$

Set $$\delta\lambda = (-N_u^T z - N)/(N_\lambda - N_u^T y) \tag{3.13}$$

and $$\delta u = z - \delta\lambda\, y. \tag{3.14}$$

Note that only systems with the coefficient matrix G_u have to be solved, so structures in G_u can be exploited. Moreover, only one factorization of G_u is needed. It has been shown [23] that even when G_u is becoming singular, Algorithm BE produces iterates that converge quadratically at limit points.

Continuation methods of various forms and levels of sophistication have been widely used in the engineering literature (see the survey [3]). For a recent survey of numerical methods for bifurcation problems, see for example the paper by Mittelmann and Weber in [19]. The approach taken here is due to Keller [12], and has recently been applied to other problems in fluid

mechanics ([7], [13] , [15], [22], [23]). A related approach suggested by Abbott [1] corresponds (in a loose way) to applying Algorithm BE to the matrix A with the last column permuted into the first n columns so that the corresponding coefficient matrix in Equations (3.11) and (3.12) becomes nonsingular even at limit points. However, as has already been pointed out, any structure or symmetry in G_u is lost in the process, and hence that approach seems unsuitable for large elliptic systems in two or three dimensions.

4. Numerical Implementation for the Internal Wave Problem

4.1 Computational Domain and Boundary Condition

The general domain of interest is the infinite strip:

$$D_\infty = (-H_2 < y < H_1 , -\infty < x < \infty) .$$

In the numerical implementation, the domain D_∞ is truncated to a rectangle of large but finite horizontal extent. If the solution obtained for such a 'box' is to represent a solitary wave, then it should not be altered if the domain is enlarged. Unless otherwise noted, this was checked numerically for all solutions calculated. The truncated domain is given by:

$$D_L = (-H_2 < y < H_1 , - L < x < L),$$

and the boundary condition is :

$$u = 0 \qquad \text{on } \partial D_L.$$

If the density stratification has certain symmetry, then the domain can be further reduced. Specifically, for the 'tanh' density profile (i.e. $F(y) = \tanh(y)$), $F'(y)$ is symmetric about $y = 0$, and it can be shown [24] that antisymetric solutions satisfying $u(x,y,\lambda) = - u(x,-y,\lambda)$ exist. Moreover, since the governing equation is invariant under a change in sign in the horizontal coordinate x, solutions symmetric about $x = 0$ exist. For such a wave, the domain D_L can be reduced to (Figure 4-1)

$$D = (0 < y < H , 0 < x < L) ,$$

and the boundary conditions become

$$u = 0 \quad \text{for } y = 0 \text{ and } H \,, \; 0 < x < L$$

$$\text{and for } x = L \qquad , \; 0 < y < H \,,$$

$$\partial u/\partial x = 0 \quad \text{for } x = 0 \,, \; 0 < y < H \,.$$

In this paper, the larger domain D_L was used so as to allow for asymmetric solutions which may exist, although none have been found so far.

4.2 Computational Mesh

Since, in most cases, most of the interesting phenomenon occurs near the origin, it would be a waste of computational effort to use a uniform grid on the domain D_L. The approach we have taken is to transform the domain D_L into another rectangular domain D_T by the following transformation (Figure 4-1) :

$$\xi = \tanh (\alpha x)$$

$$\eta = \tanh (\beta y) \,.$$

A uniform mesh in the (ξ,η) plane would put more mesh points near the origin of the domain in the (x,y) plane. The relative spacing of the mesh points in the (x,y) plane can be varied by varying the parameters α and β. Note that the inverse transformation can be obtained from the following formula :

$$\tanh^{-1} x = (\log (1+x)/(1-x)) / 2 \qquad \text{if } |x| < 1.$$

Equation (2.3) now becomes :

$$\alpha^2(1-\xi^2) \; \partial/\partial\xi \; (1-\xi^2) \; \partial/\partial\xi \;\; u$$

$$+ \;\; \beta^2(1-\eta^2) \; \partial/\partial\eta \; (1-\eta^2) \; \partial/\partial\eta \;\; u \qquad (4.1)$$

Figure 4-1: Domain, Boundary Conditions and Mesh

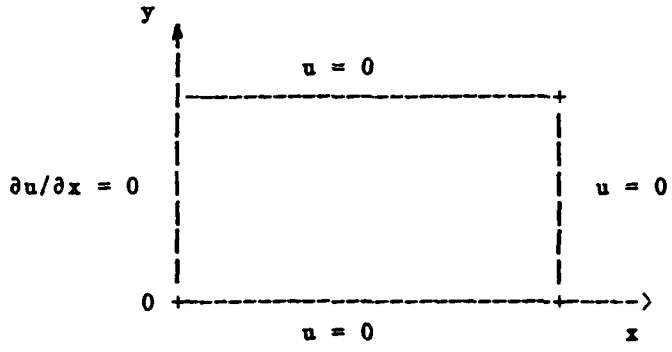

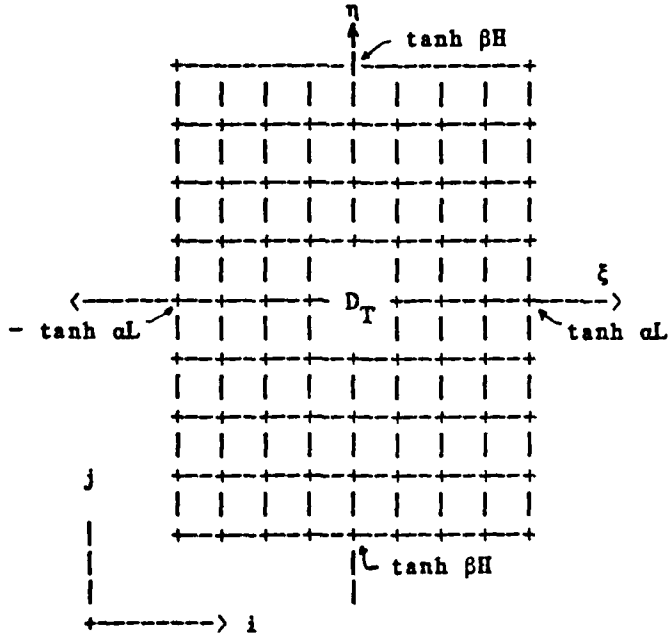

$$+ \lambda\, u\, \mathrm{sech}^2\,(u + \tanh^{-1}(\eta) / \beta) = 0 \ .$$

4.3 Discretization and Solution

To discretize Equation (4.1), we use a centered second order finite difference approximation. Let n and m denote the number of intervals in the ξ and η directions, respectively, and let

$$h = 2 \tanh(\alpha L) / n \ , \ \xi_i = \xi_1 + (i-1)\, h \ ,$$

$$k = 2 \tanh(\beta H) / m \ , \ \eta_j = \eta_1 + (j-1)\, k \ .$$

The discretized Equation (4.1) is given by :

$$\begin{aligned} (G(u,\lambda))_{i,j} &= CE_i\, u_{i+1,j} + CW_i\, u_{i-1,j} \\ &+ CN_j\, u_{i,j+1} + CS_j\, u_{i,j-1} \\ &+ (C\xi_i + C\eta_j)\, u_{i,j} \\ &+ \lambda\, u_{i,j}\, \mathrm{sech}^2(u_{i,j} + \tanh^{-1}(\eta_j) / \beta) \ , \end{aligned} \tag{4.2}$$

for $2 \le i \le n$, $2 \le j \le m$, where

$$\begin{aligned} CE_i &= (1-\xi_i^2)\,(1-\xi_{i+1/2}^2)\,\alpha^2 / h^2 \\ CW_i &= (1-\xi_i^2)\,(1-\xi_{i-1/2}^2)\,\alpha^2 / h^2 \\ CN_j &= (1-\eta_j^2)\,(1-\eta_{j+1/2}^2)\,\beta^2 / k^2 \\ CW_j &= (1-\xi_j^2)\,(1-\xi_{j-1/2}^2)\,\beta^2 / k^2 \\ C\xi_i &= -\,(1-\xi_{i+1/2}^2 + 1-\xi_{i-1/2}^2)\,(1-\xi_i^2)\,\alpha^2 / h^2 \\ C\eta_j &= -\,(1-\eta_{j+1/2}^2 + 1-\eta_{j-1/2}^2)\,(1-\eta_j^2)\,\beta^2 / k^2 \ . \end{aligned} \tag{4.3}$$

The derivatives G_u and G_λ needed in the continuation procedures can then be easily computed from Equation (4.2). The discrete operator G_u is a block-tridiagonal matrix of size (n-1)*(m-1) and has the familiar nonzero structure generated by five-point operators. Since this matrix is nonseparable, we cannot use fast Poisson solvers. Moreover, the matrix is indefinite and hence iterative methods like Successive-Over-Relaxation cannot be used directly. We have chosen to use a band solver called LEQT1B from IMSL [11]. This choice was satisfory for our problem in terms of speed and storage. Typically, L = 20 was found to be large enough to contain the solitary waves. Various values of the half-depth H were used, ranging from H = 4 to H = 40. Results from the H = 40 case was meant to be compared to experimental results obtained by Davis and Acrivos [9]. Typically, n = 20 and m = 32 was used. These were found to provide adequate resolution. All computations were performed on a CDC Cyber 176 computer, and it takes slightly less than one CPU second to obtain a solution u for a given value of λ.

5. Numerical Results

In this section, we present a sample of the numerical results that we have obtained for the internal wave problem with the 'tanh' density profile, i.e. $F'(y) = \mathrm{sech}^2(y)$. All waves presented here are 'mode-2' waves (anti-symmetric about $y = 0$) and are symmetric about $x = 0$. Other waves corresponding to different density profiles and different modes have been computed, but won't be presented here because they don't correspond to the experimental results of Davis and Acrivos [9] and probably are not as easily realizable as the mode-2 waves. More results and discussions on the fluid dynamical significance of these computed waves can be found in [24].

The dependence of u on λ as computed is shown in Figure 5-1 for $H = 4$, 10 and 40. Each value along these curves is a nonlinear solution corresponding to Equation (4.2), and many such solutions (15 to 20) are used to construct each curve.

For the shallow water case of $H = 4$, we have found nonunique solutions and a limit point at $\lambda = 0.979114$ with $(-u)_{max} = 2.647$. Some contour plots of the total stream function u+y for various values of λ are presented in Figures 5-2, 5-3 and 5-4. Contour plots for the case $H = 40$ are presented in Figures 5-5, 5-6 and 5-7.

Horizontal cross-sections cut along a line passing through the y-location

of the wave maximum are displayed in Figure 5-8. The vertical cross-sections through the same maximum are displayed in Figure 5-9. The uppermost line in Figure 5-8 is a portion of the extremely large amplitude, bore-like wave found at $\lambda = 1.1615$, past the limit point. This wave probably does not correspond to a physical solitary wave because the artificial boundary seems to have a significant influence on it. However, it does show that the mathematical problem given by Equation (4.2) has nonunique solutions. We should note here that we have not addressed the question of stability of these steady state solutions.

In Figure 5-10, the experimental results of Davis and Acrivos [9] are compared with the computed results. The density profile in their experiment can be well approximated by $F(y) = \tanh(y)$ and the half-depth is equivalent to our case of $H = 40$. The relative density change across the stratified layer in all the experiments are relatively small (i.e. σ is small in Equation (2.1)), and hence the Boussinesq approximation made to arrive at Equation (2.3) is justified. Also displayed in Figure 5-10 is the analytical result from the weakly nonlinear theory. As can be seen from the figure, excellent agreement is obtained with the fully nonlinear results of our study, even in the large amplitude and nonlinear regime, where the weakly nonlinear theory starts to deviate from observed data.

Figure 5-1: Dependence of u on λ

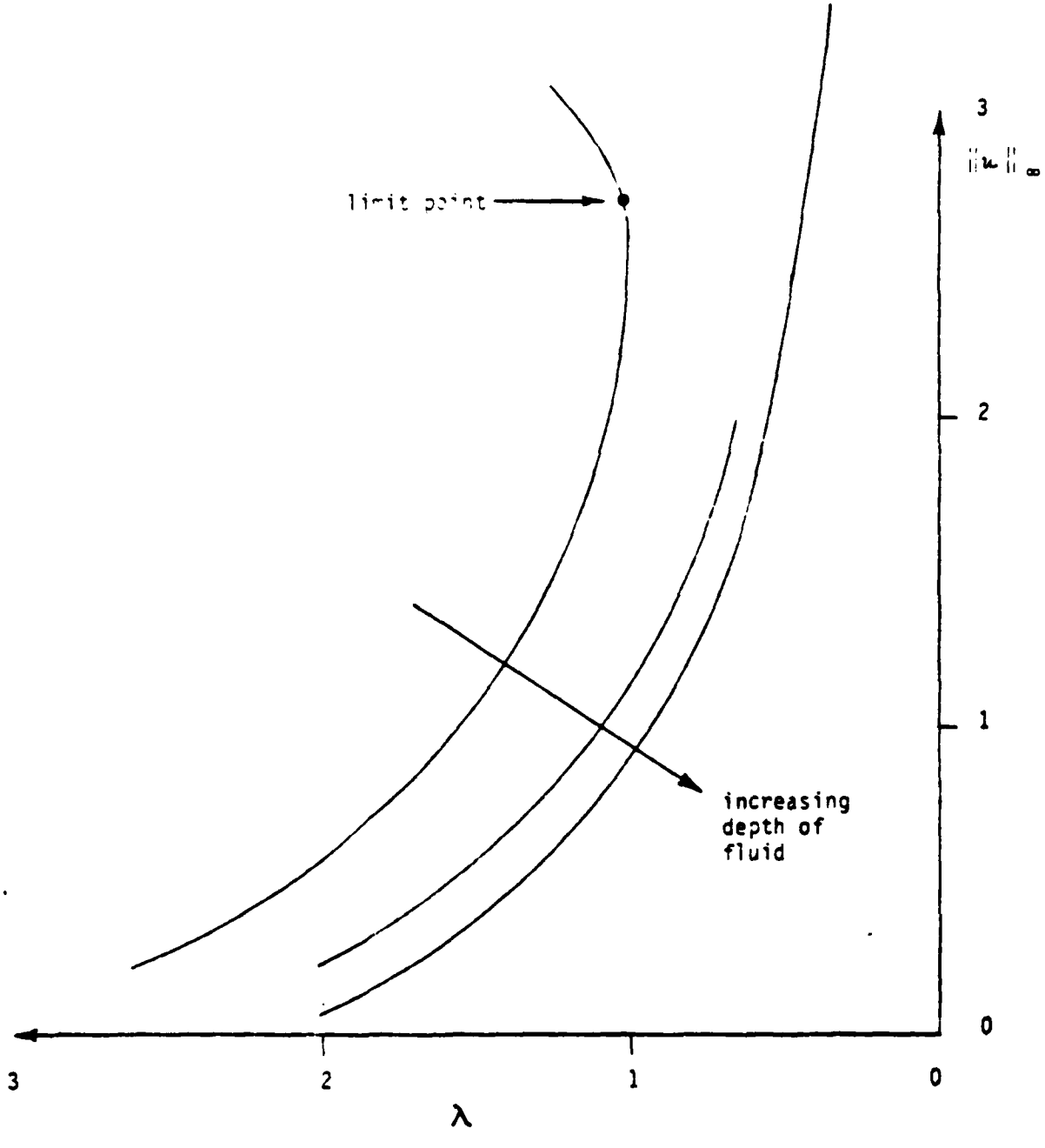

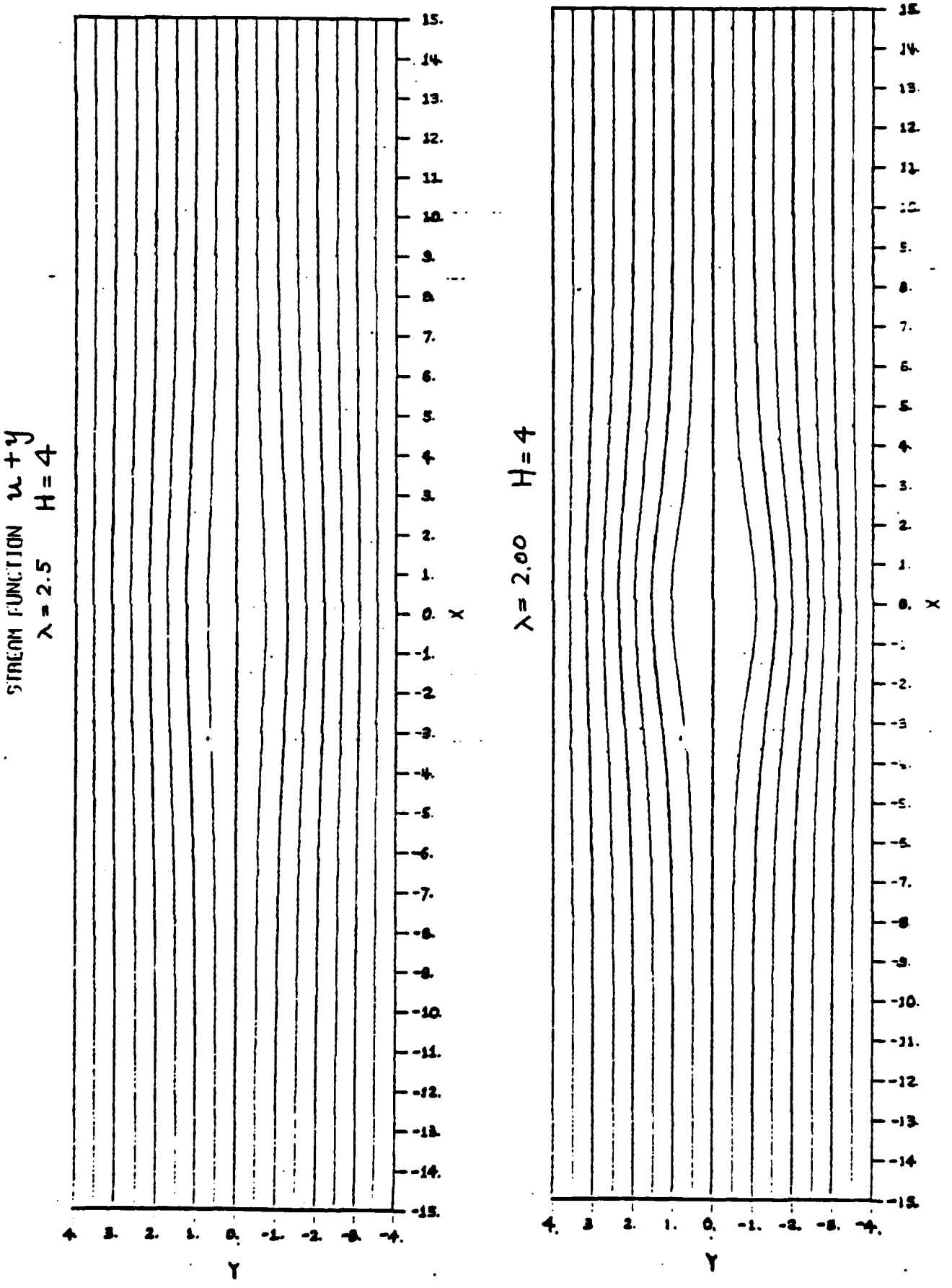

Figure 5-2: Contours of u for H = 4

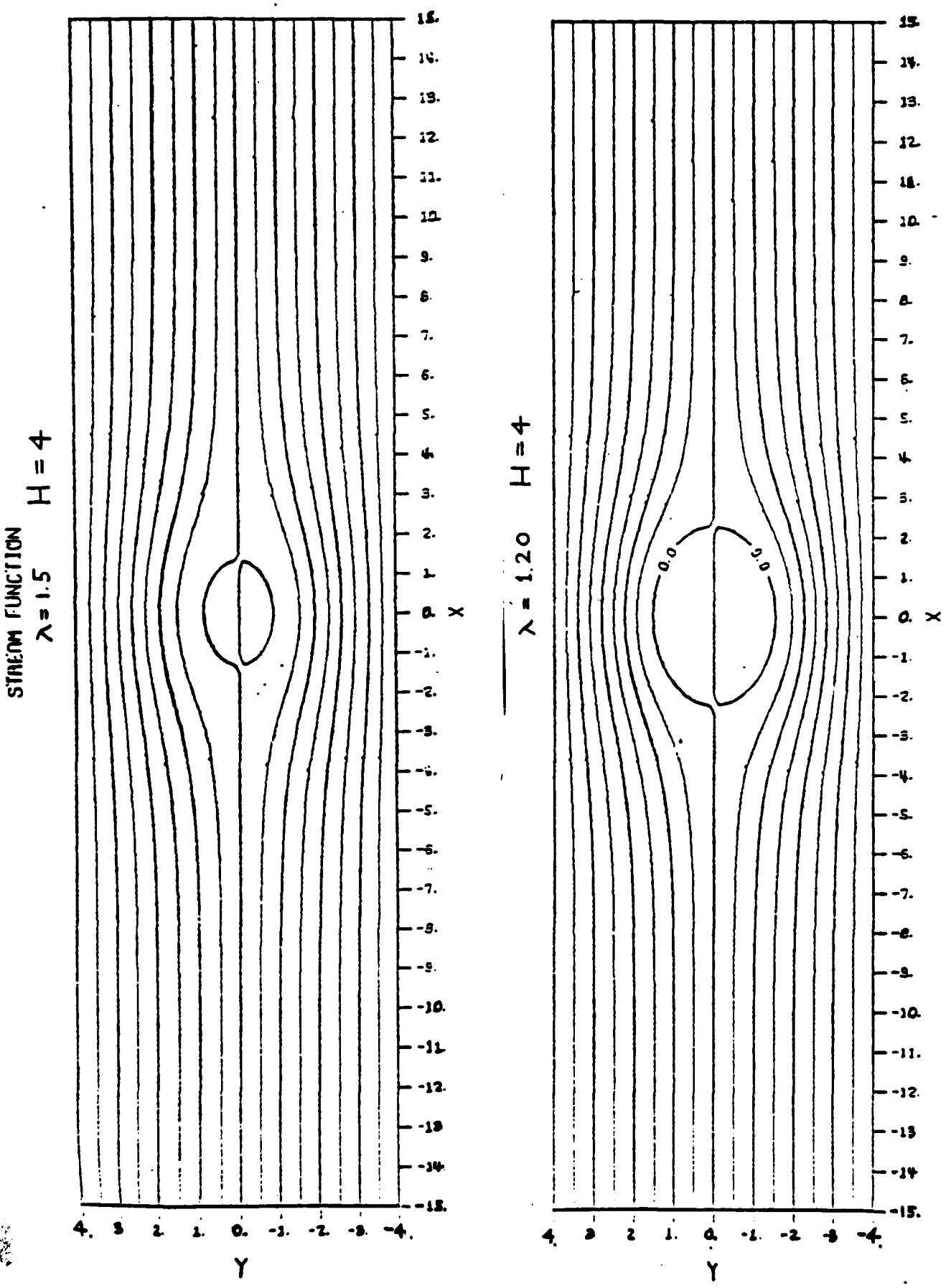

Figure 5-3: Contours of u for H = 4

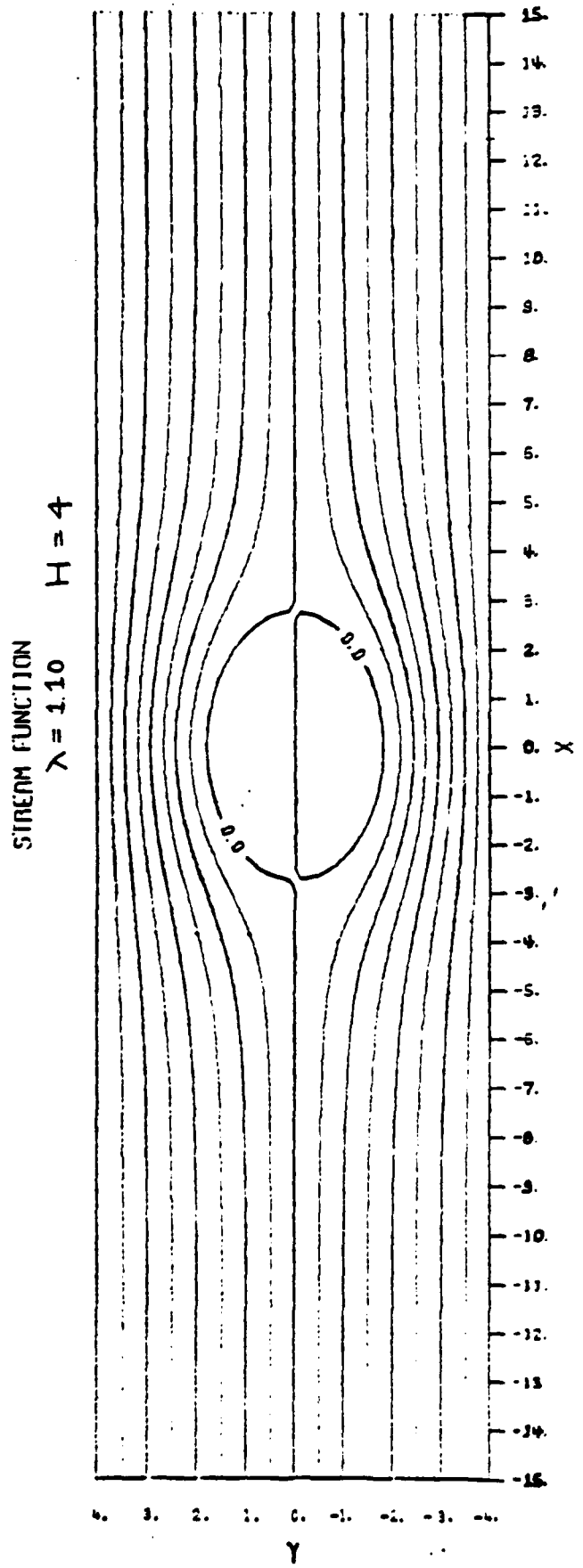

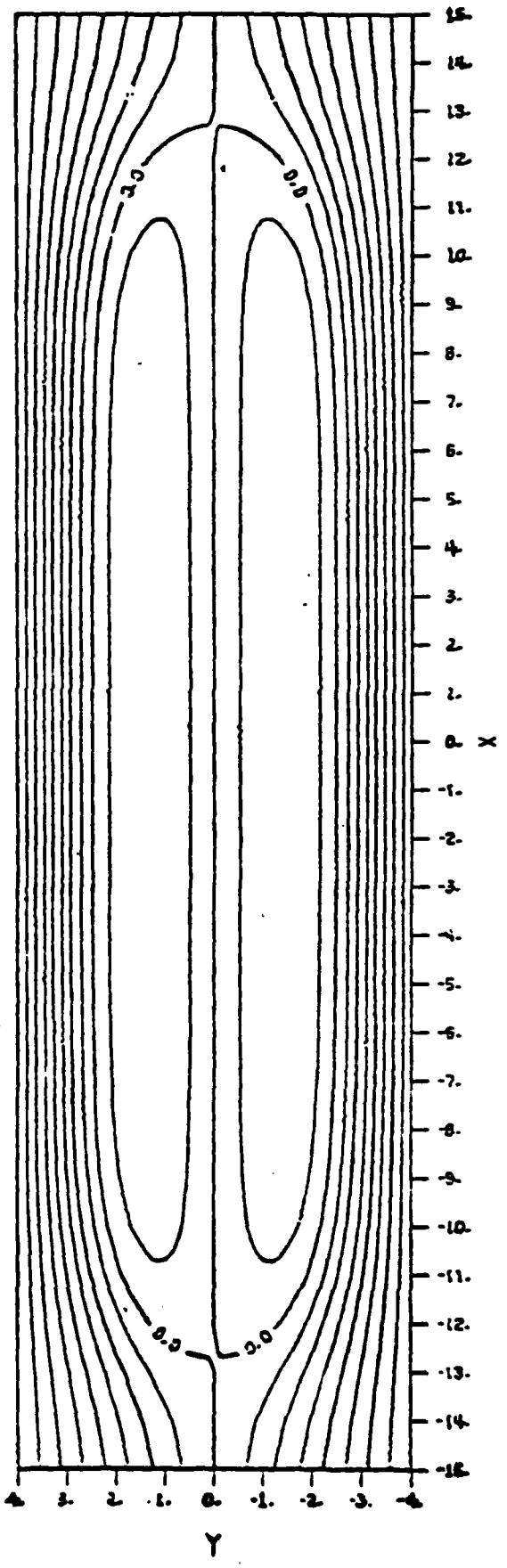

Figure 5-4: Contours of u for H = 4

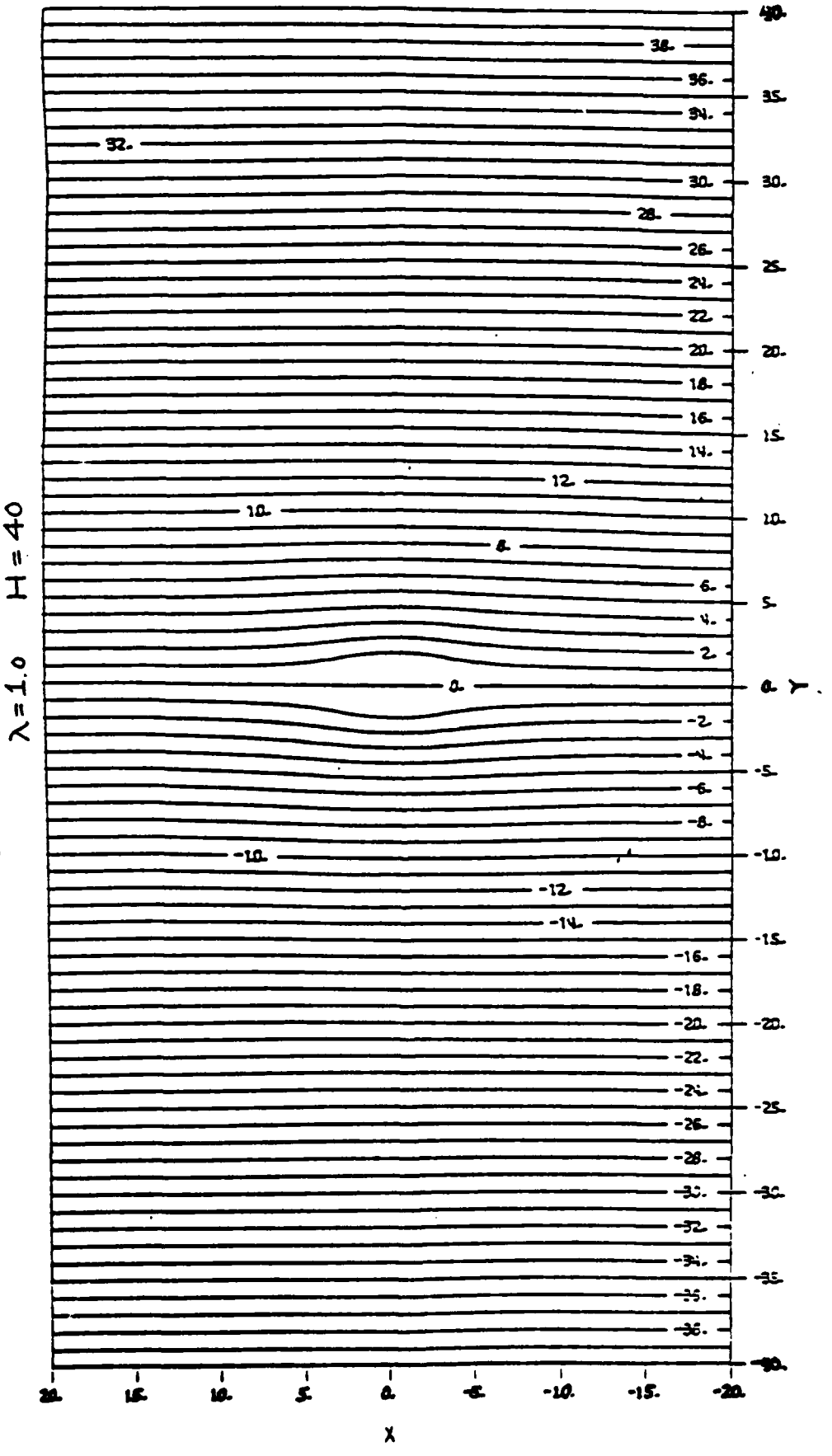

Figure 5-5: Contours of u for H = 40

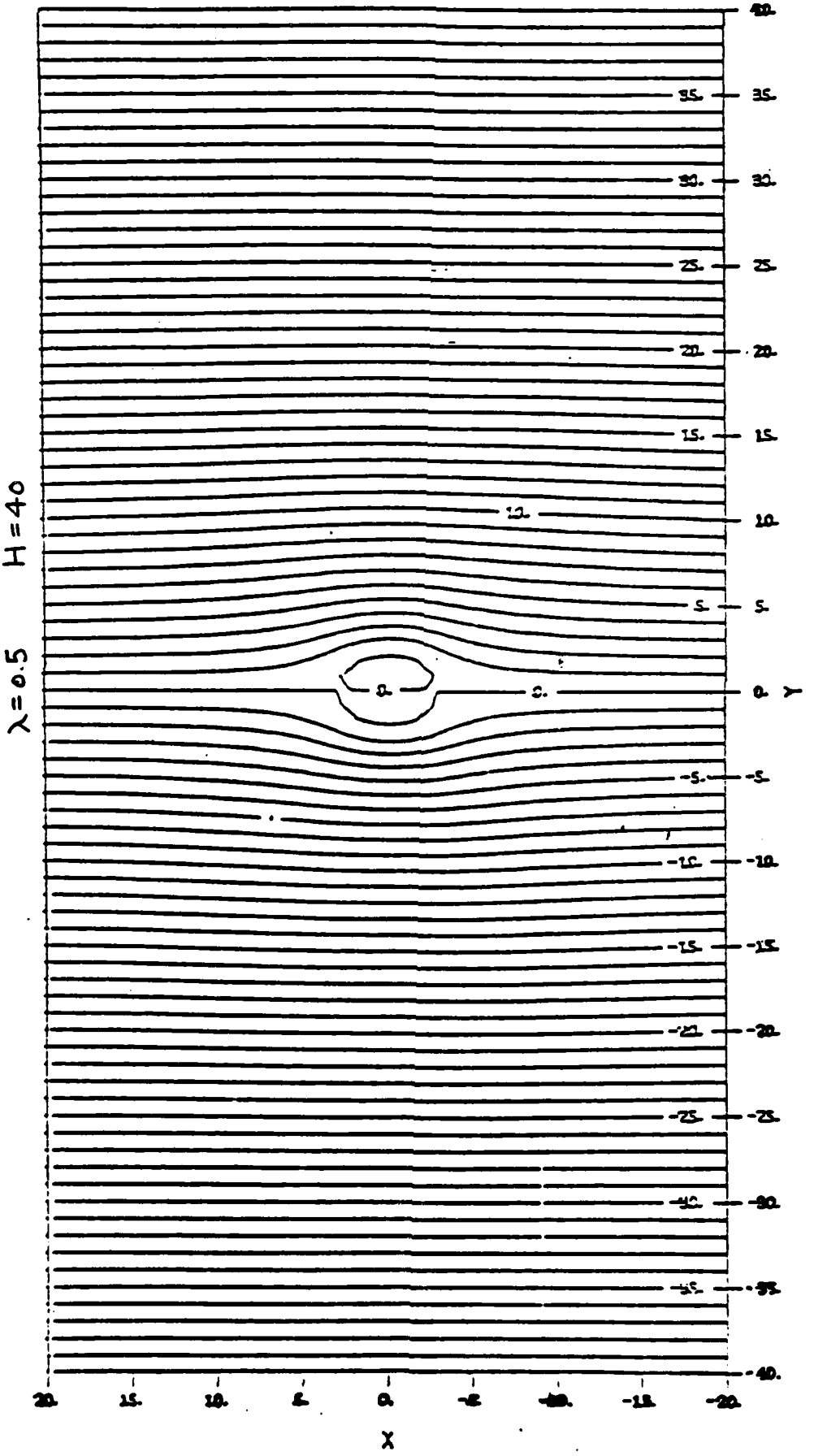

Figure 5-6: Contours of u for H = 40

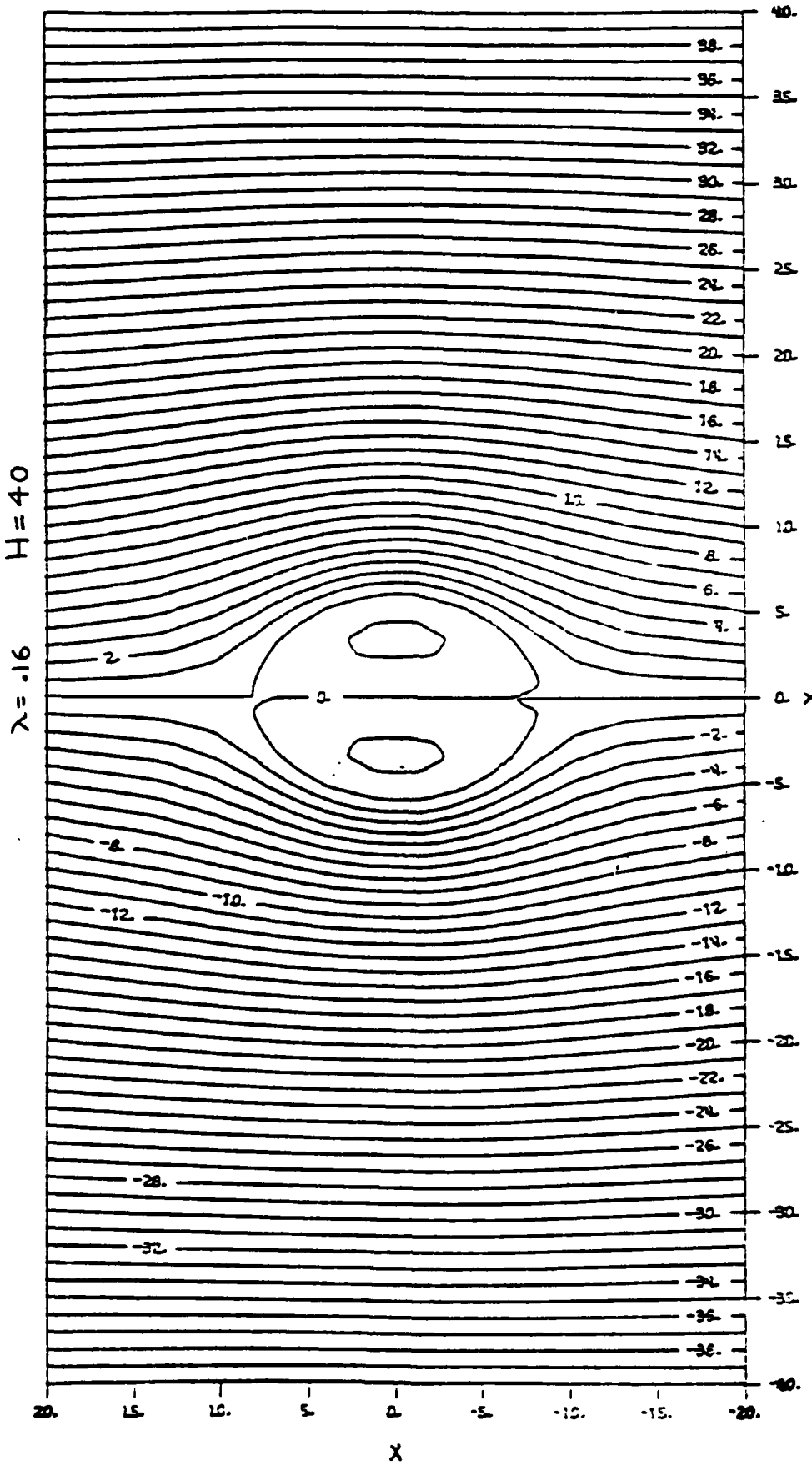

Figure 5-7: Contours of u for H = 40

Figure 5-8: X Cross-Section of u Through Maximum

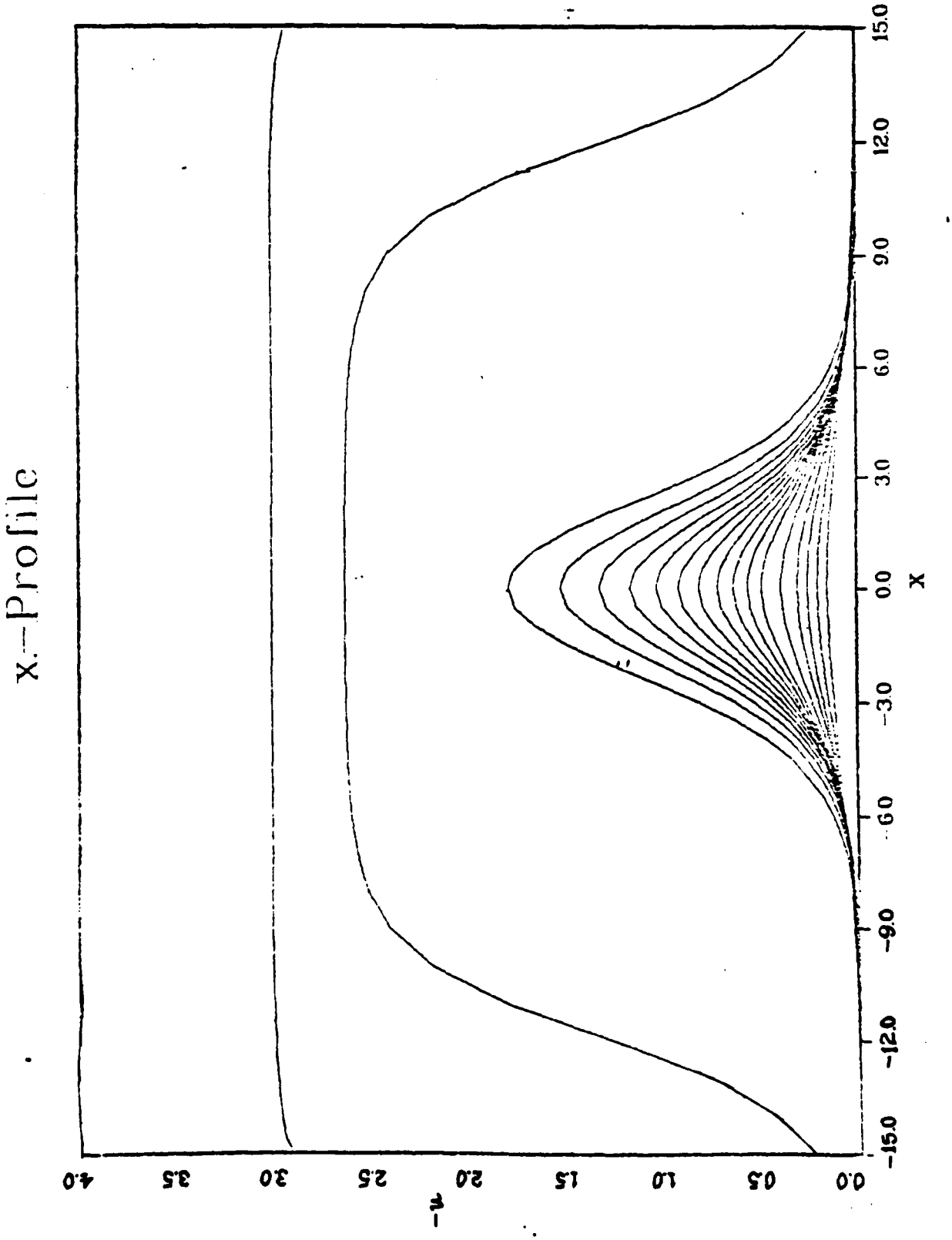

Figure 5-9: Y Cross-Section of u Through Maximum

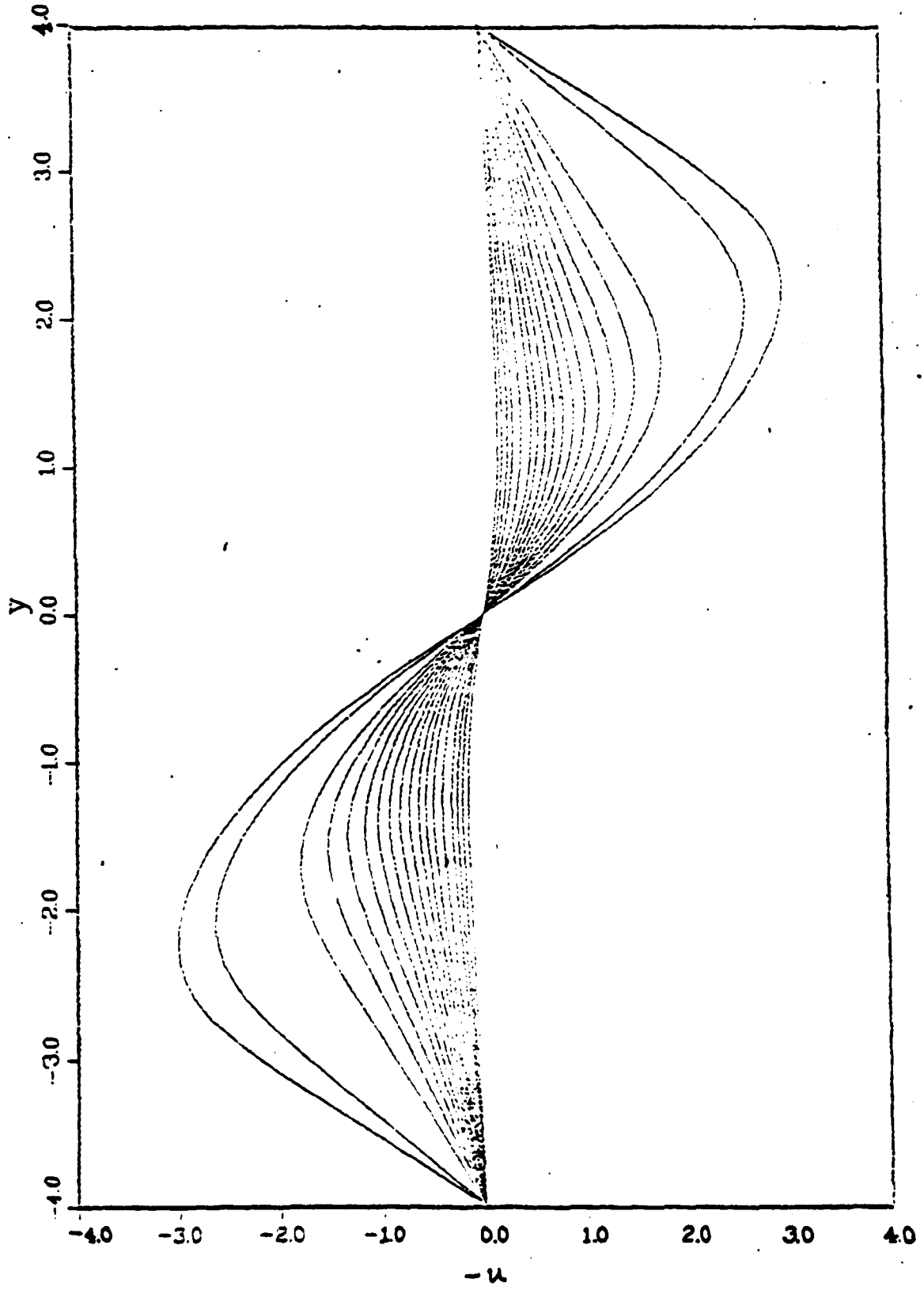

Figure 5-10: Comparison with Data of Davis and Acrivos

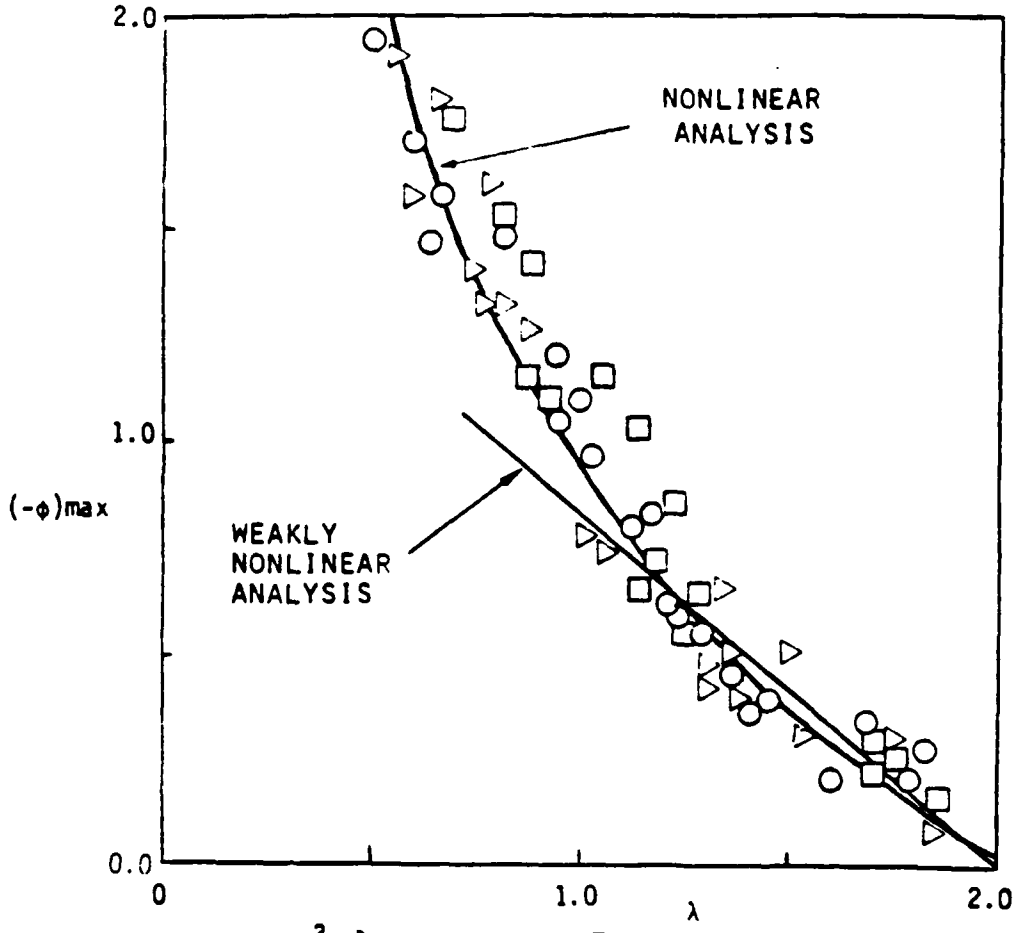

ρ_1 = 1.000 g/cm^3; ▷, ρ_2 = 1.052; □, ρ_2 = 1.095; ○, ρ_2 = 1.168

where ρ_1 = density of the fluid at the surface,
and ρ_2 = density of the fluid at the bottom.

6. Conclusion

In this paper, we described efficient continuation techniques for solving general nonlinear eigenvalue problems. We applied these techniques to the solution of Long's Equation which governs the propagation of internal solitary waves in a stratified medium. Nonunique solutions have been found by the continuation procedures. Computed results show excellent agreement with the experimental data obtained by Davis and Acrivos [9], even in the nonlinear regime where weakly nonlinear theories fail to give good predictions.

REFERENCES

[1]
J.P. Abbott, An Efficient Algorithm for the Determination of Certain Bifurcation Points, Journal of Computational and Applied Mathematics, 4 (1978), pp. 19 - 27.

[2]
M.J. Ablowitz and H. Segur, Long Internal Waves in Fluids of Great Depth, Studies in Applied Math., 62 (1980), pp. 249-262.

[3]
E. Allgower and K. Georg, Simplicial and Continuation Methods for Approximating Fixed Points and Solutions to Systems of Equations, SIAM Review, 22 (1980), pp. 28 - 85.

[4]
H. Amann, Fixed Point Equations and Nonlinear Eigenvalue Problems in Ordered Banach Spaces, SIAM Review, 18 (1976), pp. 620-709.

[5]
T.B. Benjamin, Internal Waves of Finite Amplitude and Permanent Form, J. Fluid Mechanics, 29 (1966), pp. 559-592.

[6]
D.J. Benney, Long Nonlinear Waves in Fluid Flows, J. Math. Phys., 45 (1966), pp. 52-63.

[7]
B. Chen and P. Saffman, Numerical Evidence for the Existence of New Types of Gravity Waves of Permanent Form on Deep Water, Studies in Applied Math., 62 (1980), pp. 1-21.

[8]
M.G. Crandall and P.H. Rabinowitz, Bifurcation From Simple Eigenvalues, Journal of Functional Analysis, 8 (1971), pp. 321-340.

[9]
R.E. Davis and A. Acrivos, Solitary Internal Waves in Deep Water, Journal of Fluid Mechanics, 29, part 3 (1967), pp. 593-607.

[10]

C. Garrett and W. Munk, Internal Waves in the Ocean, Annual Review of Fluid Mechanics, 11 (1979), pp. 339-369.

[11]
IMSL, International Mathematical and Statistical Libraries, Inc., Sixth Edition, July, 1977.

[12]
H.B.Keller, Numerical Solution of Bifurcation and Nonlinear Eigenvalue Problems, Applications of Bifurcation Theory, P. Rabinowitz, ed., Academic Press, New York, 1977, pp. 359-384.

[13]
H.B. Keller and R. Schreiber, Accurate Solutions for the Driven Cavity, In preparation.

[14]
T. Kubota, D.R.S. Ko and L.D. Dobbs, Weakly-nonlinear, Long Internal Gravity Waves in Stratefied Fluids of Finite Depth, J. Hydronautics, L2 (1978), pp. 157-165.

[15]
M. Lentini and H.B. Keller, The von Karman Swirling Flows, Siam J. Appl. Math., 38 (1980), pp. 52-64.

[16]
R.R. Long, Some Aspects of the Flow of Stratified Fluids, I. A Theoretical Investigation, Tellus, 5 (1953), pp. 42 - 57.

[17]
T. Maxworthy, On the Formation of Nonlinear Internal Waves from the Gravitational Collapse of Mixed Regions in Two and Three Dimensions, J. Fluid Mech., 96 (1890), pp. 47-64.

[18]
T. Maxworthy, L.G. Redekopp and P.D. Weidman, On the Production and Interaction of Planetary Solitary Waves: Application to the Jovian Atmosphere, Icarus, 33 (1978), pp. 288-409.

[19]
H.D. Mittelmann and H. Weber, Numerical Methods for Bifurcation Problems - A Survey and Classification, Bifurcation Problems and their Numerical

Solution, Workshop on Bifurcation Problems and their Numerical Solution, January 15-17, Dortmund, 1980, pp. 1-45.

[20]
H. Ono, Algebraic Solitary Waves in Stratefied , J. Phys. Soc., Japan, 39 (1975), pp. 1082- .

[21]
W.C. Rheinboldt, Solution Fields of Nonlinear Equations and Continuation Methods, SIAM J. Numer. Anal., 17 (1980), pp. 221-237.

[22]
S. Rosenblat and R. Szeto, Multiple Solutions of Nonlinear Boundary Value Problems, Studies in Applied Math., 63 (1980), pp. 99-117.

[23]
R.K.H. Szeto, The Flow Between Rotating Coaxial Disks, Ph.D. Thesis, California Institute of Technology, Pasadena, CA , 1978.

[24]
K.K. Tung, T.F. Chan and T. Kubota, Large Amplitude Internal Waves of Permanent Form in Shallow and Deep Fluid, to appear in Studies in Applied Math., 1981.

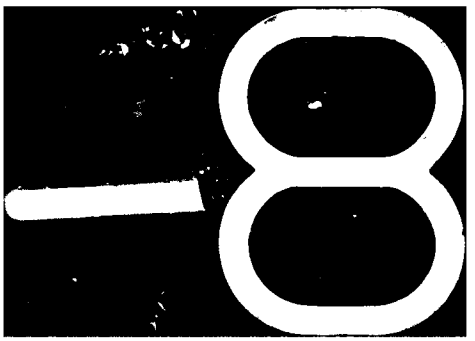
18